Geothermics 61 (2016) 12–23

Contents lists available at ScienceDirect

Geothermics

journal homepage: www.elsevier.com/locate/geothermics

Mapping alteration in geothermal drill core using a field portable spectroradiometer

Wendy M. Calvin*, Elizabeth L. Pace

Great Basin Center for Geothermal Energy, University of Nevada, MS 172, 1664 N. Virginia St, Reno, NV 89557, United States

ARTICLE INFO

Article history:
Received 24 July 2015
Received in revised form
31 December 2015
Accepted 9 January 2016
Available online 23 January 2016

Keywords:
Geothermal
Spectroradiometer
Hydrothermal alteration
Drill core
Hyperspectral
Spectroscopy

ABSTRACT

Hydrothermal alteration mineralogy in geothermal systems is commonly used to infer system temperature and past fluid flow patterns. Infrared spectroscopy is particularly good at identifying a wide variety of hydrothermal alteration minerals. The technique requires little sample preparation, and is especially helpful in discrimination among a wide range of phyllosilicate minerals that may be difficult to distinguish in hand sample or require lengthy preparation for XRD analysis. We have performed several pilot studies of geothermal drill core and chips to prototype rapid alteration characterization over large depths. These preliminary studies have established reliable methods for core/chip surveys that can quickly measure samples with high depth resolution and show the efficiency of the technique to sample frequently and provide alteration logs similar to geophysical logs. We have successfully identified a wide variety of phyllosilicates, zeolites, opal, calcite, iron oxides, and hydroxides, and note depth-associated changes in alteration minerals, patterns, or zones. Alteration mineralogy identified using these techniques shows good correlation with traditional petrographic microscope and XRD methods.

1. Introduction

Late phase geothermal exploration includes test drilling whereby a few deep wells are bored to validate temperature and permeability related to geologic and geophysical properties of the prospect. Size and depth of the borehole, and drilling methods (continuous core or rotary drilling) are elements of the exploration program that are influenced by cost as much as by the information to be gained. Continuous core provides the most geologic data possible from a drill hole, specifically information about reservoir fractures and hydrothermal alteration. However, rotary drilling is less expensive and more commonly used by the geothermal industry. Some drill holes include a combination of rotary and core operations. Rotary rigs recover geologic cuttings via the drilling fluid. Cuttings provide less geologic information regarding matrix and vein associations but are still geologically useful. We have surveyed both geothermal drill core and cuttings using infrared spectroscopy to identify alteration at depth as a means of enhancing understanding of the geothermal system, and this paper focuses on three locations for which continuous core samples were available to us.

Shortwave infrared spectral data are commonly used to identify many hydrothermal alteration minerals and precipitates that are of interest in geothermal exploration (e.g., Yang et al., 2001; Kratt et al., 2006; Calvin et al., 2015). Our group has been using this type of data since 2002 to successfully identify and map hydrothermal alteration minerals and geothermal deposits in remote sensing and field-based exploration studies (as recently summarized by Calvin et al., 2015). For these core and cuttings surveys we used our field ASD spectroradiometer with a contact probe containing an internal halogen light source.

This paper describes pilot studies we completed in an effort to define optimal data collection and processing methods, and demonstrates the effectiveness of spectral analysis of drill core for geothermal exploration. The cores used in these studies are from slimholes drilled at the Humboldt House and Blue Mountain geothermal areas in Nevada, and the Akutan geothermal area in Alaska. In the Humboldt House and Akutan examples prior detailed geochemical studies had already been performed, and their results are compared to our spectral data findings. We recommend that future studies of geothermal drill core use spectral logging as an initial survey method to refine sample locations for subsequent detailed or high-resolution geochemical analyses. In a manner similar to its use in aerial remote sensing, spectroscopy should be used as a reconnaissance tool to rapidly glean mineralogical information from downhole samples and help direct focus of later detailed studies.

* Corresponding author at: Department of Geological Sciences and Engineering, University of Nevada, MS 172, 1664 N. Virginia St, Reno, NV 89557, United States.
E-mail address: wcalvin@unr.edu (W.M. Calvin).

http://dx.doi.org/10.1016/j.geothermics.2016.01.005

2. Background

2.1. Previous work

Detailed mineralogical studies of geothermal fields have revealed a wide array of alteration minerals that are linked to the temperature, pressure, and rock type of the system (e.g., Browne, 1978; Henley and Ellis, 1983). Temperature zonation of alteration assemblages is also used in exploring for economic minerals in hydrothermal systems (e.g., Silberman and Berger, 1985). The use of these alteration facies in geothermal systems has been less well studied, particularly as it relates to borehole geology and system temperature, though several early studies explored the use of both silica and chlorites as geothermometers (e.g., Browne, 1978; Reyes, 1990). Several studies have noted alteration zonation, and that types of clay minerals (illite, montmorillonite, beidellite) can characterize temperature of alteration in geothermal systems (Guisseau et al., 2007; Inoue et al., 2004). In low-temperature systems Mas et al. (2003) found kaolinite as an indicator of current fluid pathways and kaolinite crystallinity was a tracer of fluid temperature. Specifically related to EGS stimulation, Ledésert et al. (2009) found that the presence and amount of calcite may suggest models for the chemistry of injecting fluids and the higher the calcite content the lower the natural circulation in the system. These past studies rely on time consuming sample preparation and analysis through the use of X-ray diffraction (XRD), transmission electron microscopy (TEM), and often require clay mineral separation. These studies typically survey isolated locations within the well rather than continuous measurements that could be integrated with other logging techniques.

Laboratory spectroscopic methods for mineralogy have been established for many decades. Spectroscopic methods using portable field instruments for core sample mineralogy were developed in the late 1990s (e.g., Kruse, 1996; Taylor, 2000). Studies by Taylor (2000), Sun et al. (2001), and Harraden et al. (2013) demonstrated the effectiveness of spectral measurements on a relatively small number of core samples for mineral exploration. These initial studies also noted consistency between results from spectral analysis and other geochemical methods, including XRD and X-ray fluorescence (XRF). In an early spectral analysis of geothermal samples, Yang et al. (2000) and Yang et al. (2001) measured 96 samples from Te Mihi and 285 samples from the Broadlands–Ohaaki geothermal systems in New Zealand and compared spectral results with prior studies. Most recently, automated systems have been developed to collect data at more frequent or near-continuous depth intervals and the technique is often used to better understand ore deposits (e.g., CSIRO, 2012; Tappert et al., 2011; Ross et al., 2013; see Section 5.2).

Our preliminary efforts in surveying geothermal drill core and cuttings concentrated on systematic collection of spectral data with depth at intervals of tens of centimeters to tens of meters (Kratt et al., 2004; Calvin and Solum, 2005; Calvin et al., 2010; Table 1). These pilot studies were conducted to demonstrate the value of the technique for geothermal exploration, and to establish methods that optimize speed, effort, and effectiveness. We also surveyed cuttings from the San Andreas Fault Observatory at Depth (SAFOD), and though this is not a geothermal drill hole it is included in Table 1 for completeness. As noted in Table 1, these studies surveyed from a few hundred to several thousand meters depth in data collection periods from a few hours to at most three days. We collected from 99 to 2350 individual spectra, that were then collated into depth associated databases. We analyzed these core spectra using standard methods we apply to remote sensing data sets (see Section 3.2). These initial studies helped refine the data collection and analysis methods described below. Although we collected data on cuttings for Desert Peak and Hawthorne, Nevada, the Desert Peak survey had strong interference from glue holding the chips on the board (Kratt et al., 2004). For the cuttings from the two holes at Hawthorne, Nevada these lower temperature systems did not show either the mineralogical diversity or depth-dependent changes seen in the core. Therefore, this paper focuses on the core surveys, two of which also had independent mineralogical analysis using petrographic and XRD techniques, allowing us to compare and contrast results.

2.2. Drill core locations and geology

These initial studies were conducted as unfunded demonstration projects when geothermal borehole samples were available; our surveys were not part of a planned exploration program at any of the well sites. As such, we were able to access core and chips from several locations in Nevada, as well as core from Alaska that was housed at Western Washington University. In most cases, traditional methods were used to log the lithology of the well and analyze selected cut sections, allowing us to compare our spectral data with previously published results. This paper presents detailed mineral identifications for the three well locations where core was available, Blue Mountain and Humboldt House in Nevada and Akutan in Alaska (see also Table 1).

2.2.1. Humboldt House-Rye Patch, Nevada

The Humboldt House-Rye Patch (HH-RP) geothermal area in Pershing County, is approximately 120 miles northeast of Reno, Nevada along the I-80 corridor. The site was identified in early drilling by Phillips Petroleum and has subsequently had a number of seismic and geophysical exploration activities to refine the conceptual model (Ellis, 2011). In 2003, a collaboration between the University of Nevada, Reno (UNR) and Presco Energy drilled 5 wells with core recovered from P32-2, P10-1, and P3-1. Detailed geochemistry and mineralogy of these three wells was the subject of two UNR Masters theses (Johnson, 2005; Otahal, 2006). The core was housed at UNR storage facilities where we conducted a spectral survey of P3-1 in Fall 2009, collecting 789 spectra at roughly 15 cm (~6 in) intervals over 105 m (350 ft) depth. Rock samples have since been skeletonized and are housed at the Great Basin Sample repository of the Nevada Bureau of Mines and Geology.

The general geology of the site is primarily Quaternary basin fill alluvial fan conglomerates with Pleistocene lake sediments. In P3-1, continuous core was collected below the alluvial conglomerate, from 651 to 1000 ft (198–306 m) depth. The core lithology was a sand and silt matrix-supported gravel conglomerate, with a few thin beds (<0.5 ft) of coarse sand. Otahal (2006) logged the lithology and alteration present in the core, and used petrography, SEM, XRD, and ICP-MS to characterize the geochemistry of approximately 40 samples. The area has extensive surface sinter deposits and silicification of the conglomerate was the dominant alteration noted in the core.

2.2.2. Blue Mountain, Nevada

Blue Mountain was a geothermal prospect development supported by the Department of Energy's Geothermal Technology program. The site is situated west of Winnemucca in north-central Nevada. Deep Blue No. 2 well (DB2) was an exploration slimhole well to test the commercial potential of the site. The core was the subject of a physical properties study by Ponce et al. (2009) who also presented generalized stratigraphic columns and other data synthesized from the engineering and drilling report (Fairbank Engineering, 2004). Approximately 300 reflectance spectra of core from the DB2 hole were acquired at irregular intervals in the field in May 2005. These spectra span the depth interval from 660 to 3700 ft (201–1128 m) with spot samples acquired over the course

Table 1
Summary of pilot studies conducted on drill core and cuttings.

Site	Type	Max temp. (°C)	Lithology	Depth (m)	Interval surveyed	#of spectra time to collect	Common spectral types identified
Desert Peak DP23-1	Cuttings on board	204	Tuffs, sediments, phyllite, granodiorite	0–2938	Entire length Every 20 ft	477 spectra 4 h	Chlorite, illite, muscovite, unaltered phyllite, hematite
SAFOD MHST1	Cuttings	n/a	Sediments, granite, granodiorite	0–4000	Entire length every 100 ft	199 spectra 1/2 day	Weakly altered, smectite clays (montmorillonite)
Blue Mountain DB2	Core	167	Argillite, phyllite, dacite	201–1128	Uneven interval	297 3 days	Phyllite, montmorillonite/illite, hydrated quartz/opal, chlorite + montmorillonite, serpentine + prehnite, carbonate
Humboldt House HHP3-1	Core	110	Conglomerate—silicified or mud/sand supported	198–306	Entire interval systematic, every ~15 cm	789 2 days	Weakly altered mafics, illite/chlorite, hydrated quartz/opals, kaolinite, jarosite
Hawthorne HWAAD-2	Cuttings	49	Alluvium, sandstone, and granite	0–1437	Entire interval systematic	446 1/2 day	Montmorillonite, montmorillonite + illite + chlorite, chlorite + epidote
Hawthorne HWAAD-3	Cuttings	43	Aluvium, sandstone, and granite	0–1175	Entire interval systematic	405 1/2 day	Montmorillonite, montmorillonite + illite + chlorite, chlorite + epidote, carbonate
Akutan HSB2	Core	162	Basalt, andesite, ash tuff, lithic basalt	0–254	Uneven interval with focus on alteration	1499 6 h	Zeolites, epidote & prehnite, calcite, muscovite, kaolinite
Akutan HSB4	Core	160	Basalt, andesite, ash tuff, lithic basalt	0–457	Uneven interval with focus on alteration	2350 8 h	Zeolites, calcite, muscovite, kaolinite

of 3 days as the core was transported from the core shed at the drill site to pallets for warehouse storage.

The drill hole penetrated Jurassic and Triassic metasedimentary rocks predominantly consisting of argillite, mudstone, and sandstone, and Tertiary diorite and gabbro, with mafic intrusive rocks throughout the lower section of the hole. Ponce et al. (2009) analyzed 46 samples from the DB2 hole for density, porosity, and magnetic susceptibility. To our knowledge no other geochemical analyses have been performed.

2.2.3. Akutan, Alaska

Akutan, Alaska is a remote Aleutian island where power is generated by costly imported diesel fuel and the community is interested in developing local sources of energy production (Kolker et al., 2012). As part of a phased geothermal energy exploration and development plan, two slimholes, HSB2 and HSB4, were drilled to 833 ft (253 m) and 1500 ft (457 m) depths in 2010, with continuous core collected from both holes (Kolker et al., 2012). Stelling and Kent (2011) completed a thorough study of the HSB2 and HSB4 cores using 60 petrographic thin sections, XRD, and SEM. The full drill core was housed in offices and warehouse space at Western Washington University in Bellingham, Washington. Reflectance spectra were collected from the full length of both drill holes resulting in over 3000 spectra collected in the span of two days in spring 2012. The sampling interval was dense, but irregular, focusing on obvious alteration minerals.

The Akutan volcano is historically very active and the lithology of the slimhole cores is dominated by basalt and lithic basalt with areas of andesite and thin regions of tuff. Stelling and Kent (2011) selected samples based on depth and abundance of fractures, mineralization, and alteration, and they identified up to 16 different geothermal indicator minerals within the core samples, including zeolites, secondary minerals, and clays. Littlefield et al. (2012) presented the initial comparison of the spectral mineral analysis results with the previous petrographic analysis.

3. Methods

3.1. Data collection

We used an Analytical Spectral Devices, Inc., (ASD) FieldSpec Pro portable spectroradiometer to collect data from 0.35–2.5 μm. This wavelength range spans the visible/near-infrared to shortwave infrared regions of the electromagnetic spectrum, often called VNIR/SWIR. The spectral resolution of the instrument is 3–10 nm, sufficient to identify common mineral absorption features at these wavelengths, and the default collection mode is to record spectra at 1 nm intervals, significantly oversampling the instrument resolution. Initial studies (Desert Peak, SAFOD, and Blue Mountian-DB2) used an external light source and standard 8-degree field of view objective. Later studies utilized an ASD contact probe with an internal halogen light source. The field of view for the contact probe is 10 mm in diameter. Both collection methods obtain spectral data that are representative of the mixture of minerals within the instrument field of view. Spectra are acquired on the outer (rounded) edge of core and if the core is naturally split, spectra of interior faces may be obtained. The ASD instrument is calibrated against a halon plate at the start of and periodically throughout data collection, so that data are reported in reflectance for direct comparison with established mineral spectral library standards.

Data are collected throughout the length of the core, be it at a specific depth interval (e.g., every 10 ft) or at areas of interests (e.g., highly fractured) or both. For example in the Akutan core, spectra were mostly collected in visibly altered and mineralized sections of core, and some representative spectra were collected from the unaltered rock (Littlefield et al., 2012). Spectra are displayed on the instrument control laptop in real time during data collection so the researcher may decide to collect data from a sample that has an interesting spectrum at first glance. If, at the time of drilling, basic lithology was logged or core photos were taken, the researcher may use this information to design the data collection plan to focus on specific depth intervals of interest.

Time available for data collection also factors into the interval at which core are sampled and the focus of the survey. With the exception of the SAFOD study, in each of the pilot studies we took our field instrument to a warehouse, laboratory, or off-site location to perform the data collection (we went to the samples rather than shipping the samples to UNR's spectroscopy lab). These pilot studies were also not conducted in geologic core repositories so that equipment such as core rollers, or warehouse support staff to move samples, were not available to us. In all cases our goal was to sample major features over large sections of core in as short a time as possible. Because the data collection is rapid (a few seconds per spectrum) the data can be gathered quickly and analyzed in detail at

a later time. Moving the core boxes and detailed note taking are the most time consuming parts of the activity and it is helpful to have a few able bodies to set up an assembly line to move boxes under the spectroradiometer somewhat rapidly. A small team of two to four has worked well, one running the instrument, one keeping detailed notes relating spectral acquisition number to core box number, and ideally two to move core boxes. In a core repository setting acquisition is expected to be even more streamlined and require fewer people.

3.2. Data processing

Reflectance spectra are recorded as individual files with a unique number appended. We first build a database that links the spectrum number to the depth so that spectra can be stacked in order of location in the well. This is done because, depending on the organization of core boxes, spectra are not always collected in depth order. Data are corrected for spike offsets that commonly occur along instrument detector boundaries (detector splice correction) and output as text files using ASD's ViewSpec software. Custom code developed by the authors in IDL converts individual spectra into an image "cube" where the impression of width is provided by repeating the spectrum across a horizontal row, and vertical dimension in the image is depth in the well (Fig. 1, Calvin et al., 2010). In order to use ENVI statistical image processing routines developed for remote sensing data, the core data must be reduced to 5 nm spectral sampling interval. This was accomplished by performing a boxcar smoothing on the original spectrum. This reduces the number of channels but does not alter the appearance of absorption features, as the instrument is already oversampling relative to the instrument resolution, as described above. We then use a combination of statistical and experience based processing routines to identify common spectral features observed in the data and relate these to known alteration minerals (e.g., Calvin et al., 2015, Section 3.3). Fig. 1 provides an example of the DB2 core, showing an initial map with depth.

Due to the spot size of the spectroradiometer, spectra in the core survey are typically combinations of several minerals, and we associate common core spectral types with known alteration minerals or mineral assemblages using established spectral libraries (e.g., Clark et al., 2007) or the Spectral Assistant contained in TSG (The Spectral Geologist) which is a commercial software package developed by the Commonwealth Scientific and Industrial Research Organization (CSIRO) of Australia. Thus at a particular depth, several minerals might be identified due to multiple diagnostic features. We can then plot individual minerals found at a particular depth in a horizontal display against lithology as is commonly done to explore changing alteration patterns with depth in geothermal drill holes (see Section 4). In practice we have found that while automated methods do a reasonable job of identifying dominant minerals in the spectrum, in some situations spectra may be misidentified, or mineral assemblages might not be uniquely separable. Thus additional inspection by an analyst familiar with mineral spectroscopy is an important part of the depth map validation.

3.3. Spectral identification of minerals and mineral assemblages

Because the contact probe measurement provides data in the 1.4 and 1.9 μm regions, wavelengths that are obscured in traditional remote sensing studies by atmospheric water vapor, it is worthwhile to briefly review the spectral properties of common alteration minerals we have identified in these pilot studies. Additionally, the spectra are nearly always mineral mixtures so that core spectra can exhibit several features that vary in relative strength and express

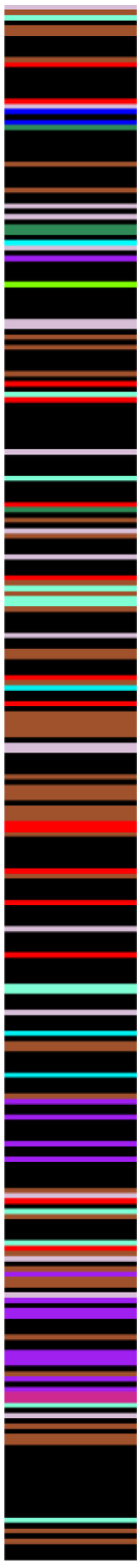

Fig. 1. Example of mapped minerals in a core spectral stack for DB2. Each row represents one measurement. Brown is unaltered or lightly altered, purple is carbonate, shades of cyan and light green are mixed Fe–Mg muscovite/illite/chlorite, blue is hydrated quartz, red is opal, chartreuse and dark green are Al-phyllosilicates. Areas that are black are unmapped or not well matched to initially identified alteration spectra. See Section 3.3 for representative spectra.

locally changing compositions or changes in the relative abundance of dominant minerals in the field of view.

3.3.1. Aluminum phyllosilicates (illite, kaolinite, montmorillonite/smectite, muscovite)

Also sometimes referred to as "2.2 μm clays" due to the strong absorption due to Al-OH near that wavelength, spectra of pure minerals in this category have been presented by Clark et al. (1990), Gates (2005), and Bishop et al. (2008). These minerals commonly have strong absorption at 1.4, 1.9, and 2.2 μm as shown in Fig. 2. Kaolinite, commonly identified in numerous remote and in situ studies, has a characteristic asymmetric doublet at 2.2 μm. The features in montmorillonite are broad and asymmetric with steep slopes on the short wavelength side of the 1.4 and 1.9 features. We use montmorillonite as a common smectite clay, but the spectral shapes are similar to and may represent other smectites such as beidellite (Bishop et al., 2011). Illite has features between montmorillonite and muscovite, with an additional feature near 2.35 μm, and noticeably different shape and weaker feature at 1.4 (narrow on the short wavelength side). Muscovite is characterized by a trio of features between 2.2 and 2.5 μm, the strongest at 2.2, with two other broad features near 2.35 and 2.45 μm. Small variations in the band center at 2.2 μm are noted in hydrothermal systems related to ore deposits as muscovite transitions to phengite (e.g., Yang et al., 2011; Tappert et al., 2013). The substitution of Si(Mg,Fe) for Al shifts the band from 2.195 to 2.225 (Yang et al., 2011; Tappert et al., 2013), though Yang et al. (2011) noted that active geothermal systems do not appear to have a consistent relationship between composition and either temperature or pressure. The library spectrum shown in Fig. 2c has a band center at 2.215, tending toward the phengite direction of what is a continuum of band center position (e.g., Yang et al., 2011). In our pilot studies we did not observe strong changes in the band centers of this feature, and use here the term "muscovite" to refer to these features as no spectra at the longest wavelengths were noted. The majority of library kaolinite samples have two shallower features at 1.805 and 1.935 μm; however we find in our pilot studies the 2.2 μm doublet is often accompanied by an asymmetric 1.9 μm band, more similar to montmorillonite and illite. This 1.9 μm spectral shape may be related to close intergrowth of kaolinite with other aluminum phyllosilicates. In core spectra the 2.2 μm kaolinite doublet may be more or less expressed, often appearing as simply shallower feature with a change in slope on the short wavelength side of the absorption envelope. The asymmetry is still characteristic of kaolinite, even if the short wavelength portion of the doublet does not have a defined minimum. Minerals in the alumino-phyllosilicate group are common in argillic and phyllic alteration zones in a variety of environmental settings (Thompson et al., 1999). Additionally, the presence of smectites is associated with "a clay cap" that can seal a geothermal reservoir and has high conductivity that is often the target of magnetotelluric surveys, and the transition from montmorillonite to illite may indicate a high temperature reservoir beneath the "clay cap" (e.g., Gunderson et al., 2000; Newman et al., 2008).

3.3.2. Fe–Mg phyllosilicates (chlorite, clinochlore) with epidote

Propylitic alteration zones are common in epithermal ore settings and are characterized by chlorite, epidote, sericite (muscovite/illite), actinolite, and zeolites. (Thompson et al., 1999). Spectra of pure minerals in this category have been presented in numerous publications (Clark et al., 1990; King and Clark, 1989; Calvin and King, 1997; Bishop et al., 2008). This combination of minerals is common in our pilot studies, regardless of the host system lithology (Section 2.2). With this group of minerals core spectra tend to fall into two groups, those with a boxy or square-shaped 1.9 μm feature and those with a more pointed or triangular feature. Figs. 3 and 4 demonstrates these features as mixtures of muscovite, illite and chlorite and/or clinochlore, and epidote (MICE) that together create a common suite of features, at 2.20, 2.25, and 2.35 μm, but whose relative strengths and absolute band centers vary throughout the core stack as the proportion of each mineral in the spectroradiometer field of view varies. Illite/chlorite mixtures were also noted with similar triplet features at Te Mihi in the Wairaki system in New Zealand (Yang et al., 2000). Additional variation, such as the presence of a well-defined narrow feature on the short wavelength side of, or within, the 1.9 μm envelope is also present in these mixtures. In order to obtain a more triangular 1.9 μm feature, some amount of a smectite (such as montmorillonite) needs to be included in linear combinations as shown in Fig. 4.

3.3.3. Silicates: prehnite, hydrated quartz, opal, zeolite

In hydrothermal alteration of host rocks, adularia and other potassium feldspars and quartz commonly occur. Unfortunately many of the major rock forming silicates do not have absorption features at the short infrared wavelengths. However, water or hydroxyl in the mineral structure will create diagnostic absorption features for some silicates, including prehnite, opal, and zeolites.

In a single location in the DB2 core and commonly throughout the HSB2 core, we identified prehnite. This mineral, which marks a transition zone in temperature and pressure in the metamorphic facies scale between zeolite and greenschist, indicates higher temperatures and relatively low pressure. In hydrothermally altered basalts, it is commonly found with zeolites, and it has been identified in studies of geothermal fields in Iceland, Lesser Antilles, and Kamchatka (Marks et al., 2010; Mas et al., 2006; Kralj and Rychagov, 2010). Though occurring with zeolites and other Ca-silicates, the spectral properties are more similar to the phyllosilicates. Infrared spectra of prehnite in the wavelength range we measure have been presented by Ehlmann et al. (2011). Fig. 5 shows spectra of prehnite identified in the DB2 and HSB2 cores compared to the pure mineral spectrum from the USGS library (Clark et al., 2007). Prehnite is identified by the unique location of a narrow feature at 1.48 μm, with multiple features at longer wavelengths that can be diagnostic if relatively unmixed (HSB2 examples), however we often see prehnite mixed with chlorite as in the DB2 spectrum.

Also commonly occurring in our drill core data are the spectral features of hydrated quartz, opal, and zeolites. While quartz is not expected to have features at these wavelengths, in surveying the DB2 core, several notable quartz veins were apparent in the core, and measurement of these veins resulted in spectra similar to opals, but without a 2.2 μm feature. Subsequent laboratory measurement of the sample confirmed the diagnostic quartz features near 10 μm, so it is inferred that fluid inclusions result in the appearance of the short wavelength spectrum shown in Fig. 6. Hydrated amorphous silica (opal) is commonly mapped in our surface remote sensing studies and appears similarly in the core surveys. Both the hydrated quartz and opal are characterized by broad and symmetric features centered on 1.4 and 1.9 μm associated with water. In addition, opal has a broad diagnostic band or stair step at 2.2 μm (e.g., Goryniuk et al., 2004). The spectra of many zeolites (stilbite, laumontite, clinoptilolite, heulandite) are similar to each other, while analcime and natrolite have additional features that make them diagnostically identifiable using this technique. Zeolites similar to heulandite are shown in Fig. 6b, and their spectra are similar to the hydrated quartz, but with narrower and more asymmetric features. Additional water absorption bands near 1.0 and 1.2 μm are also often present with the zeolites.

3.3.4. Carbonates

Calcite is common at a wide range of temperatures in geothermal fields. If the host rock lithology includes carbonates it may be a source of CO_3 remobilized by hydrothermal fluids, and CO_2-

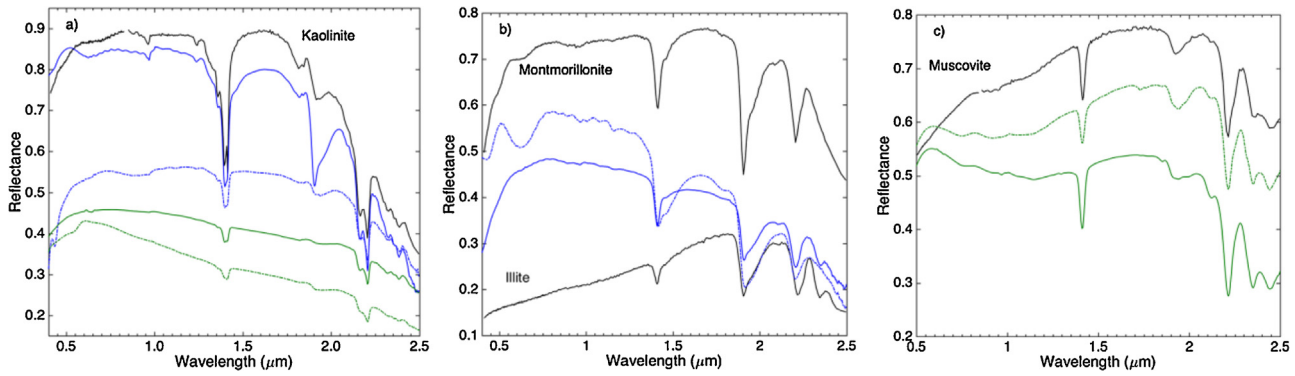

Fig. 2. Example core spectra and identified mineralogy. In each panel, black lines are well-characterized pure minerals from the USGS (Clark et al., 2007), blue lines are from Blue Mountain DB2, green lines are from Humboldt House P3-1. (a) Kaolinite, (b) illite/montmorillonite, (c) muscovite. These core spectra were selected as best representative of single minerals, though many core spectra have subtle gradations among relative strength of the features.

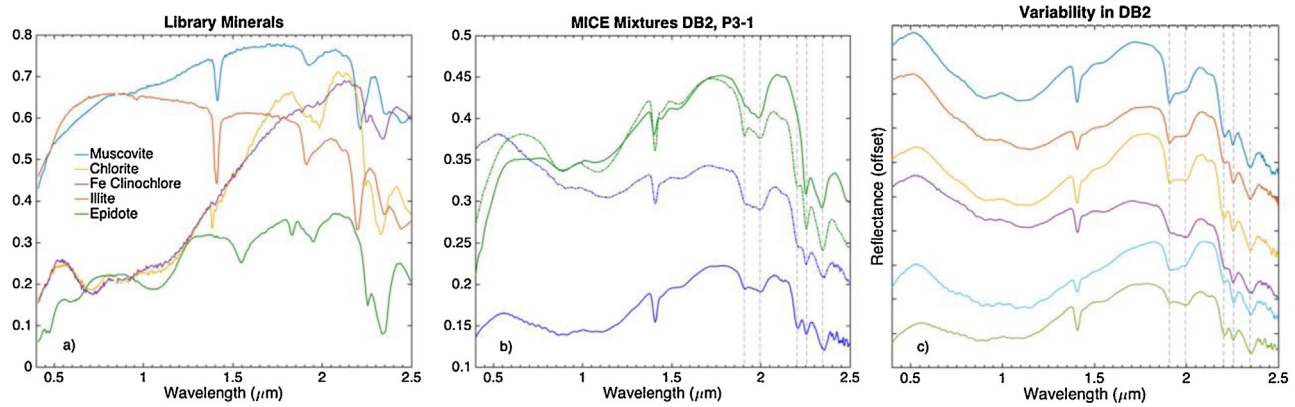

Fig. 3. (a) Library spectra of muscovite (blue), illite (orange), and chlorite (yellow), and ferroan clinochlore (purple), and epidote (green) (MICE). Fig. 4a shows mixtures of these minerals. (b) MICE mixes in DB2 (blue) and P3-1 (green), with boxy 1.9 μm features. Vertical dashed lines call attention to absorption features that vary in relative strength. See also the discussion in the text. (c) Plot of variability in relative strength of MICE diagnostic features in DB2 (spectra offset for clarity).

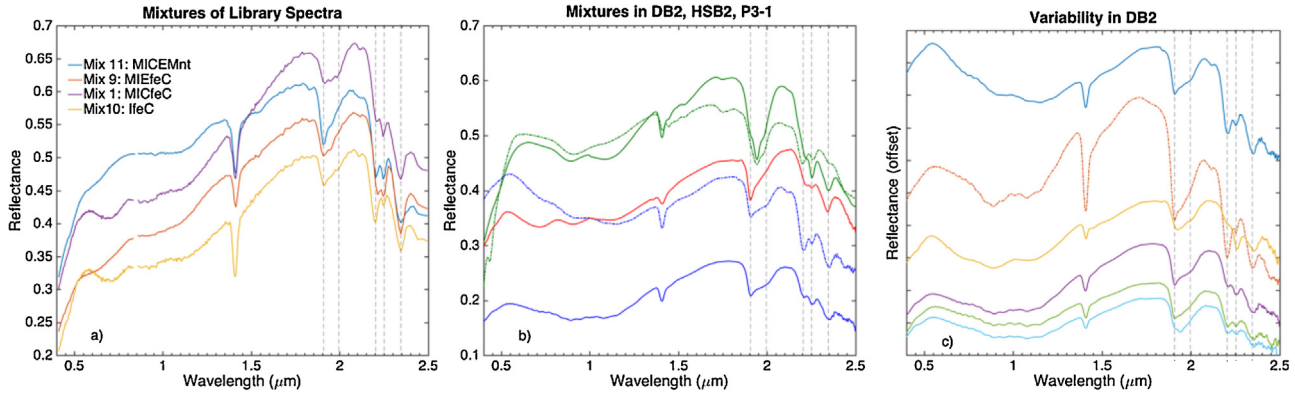

Fig. 4. (a) Various linear mixtures of library spectra including muscovite (M), illite (I), chlorite (C), ferroan clinochlore (feC), epidote (E), and montmorillonite (Mnt), showing the characteristic triplet described in the text and identified with dashed vertical lines at 2.20, 2.25 and 2.35 μm. Depending on the mineral combination, common features observed in core spectra are replicated, including varying relative strength of the triplet features and boxy or triangular 1.9 μm feature shapes. (b) Spectra from DB2 (blue), P3-1 (green), and HSB2 (red) with triangular 1.9 μm features. (c) Plot of variability in relative strength of features in DB2 (spectra offset for clarity).

saturated waters will deposit carbonates as hot fluids rise and boil, and CO_2 comes out of solution in the gas phase (Fournier, 1985). The spectral features of carbonates and the impact of cation substitutions have been documented in classic early work by Gaffey (1986, 1987). We identified calcite throughout both the DB2 and HSB2 cores, with representative spectra shown in Fig. 7. Gaffey (1986) demonstrates that very small amounts of iron will impact the strength and appearance of the two features between 1.8 and 2.0 μm and contribute a large broad feature centered near 1.25 μm.

4. Results and comparison to prior studies

4.1. Humboldt House (P3-1)

Four minerals were identified in the P3-1 core, kaolinite, opal, chlorite, and muscovite (Fig. 8). The chlorite and muscovite generally occur as a mixture, which is why their spatial distribution with depth is correlated, as shown in Fig. 8. This chlorite-muscovite mixture is pervasive throughout the entire length of the core. Otahal

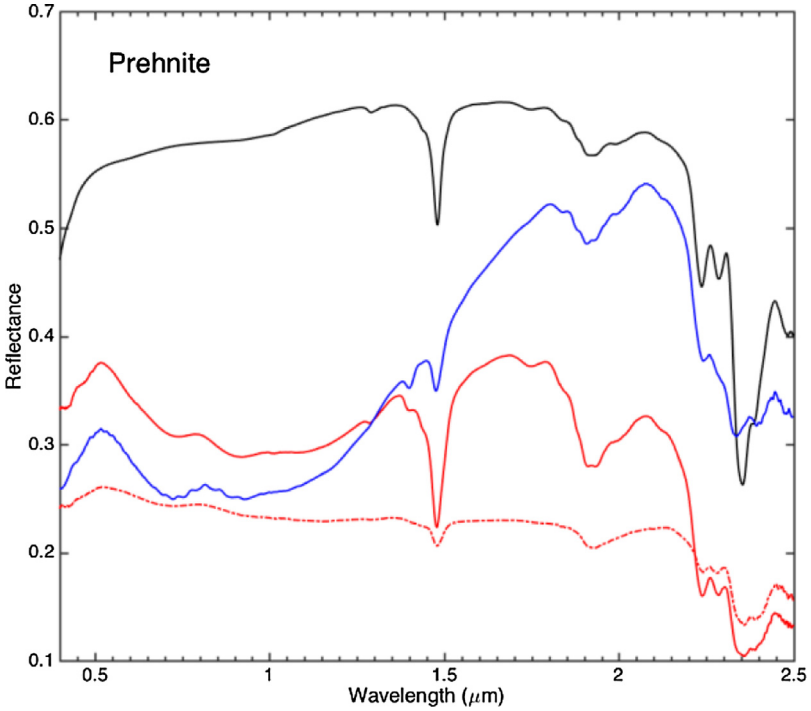

Fig. 5. Characteristics of prehnite from DB2 (blue) and HSB2 (red) cores compared with a library spectrum (black).

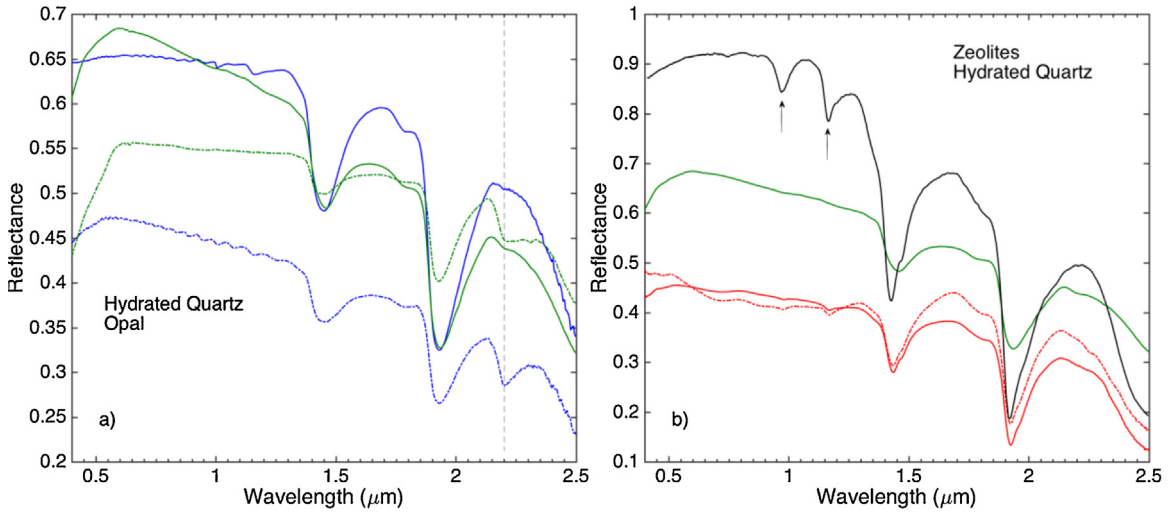

Fig. 6. (a) Spectral characteristics of hydrated quartz (broad features without a 2.2 μm band), and opal (with a 2.2 μm band), from the DB2 (blue) and P3-1 (green) surveys. High frequency "ringing" at wavelengths less than ~1.25 μm in DB2 is an artifact of the data collection technique that is eliminated when using the contact probe as described in Section 3.1. (b) Characteristic features of zeolites as represented by heulandite from the USGS library (black), and as seen in the HSB2 core (red). The hydrated quartz from P3-1 is repeated from 6a (green) to easier see the narrower features, relative asymmetry and additional features at 1.0 and 1.2 μm that typify zeolites.

(2006) examined 52 samples using XRD and identified quartz, chlorite, muscovite, pyrite, kaolinite, halloysite, illite, dickite, and barite. Two main alteration events were outlined, the first advanced argillic alteration noted by relic textures of bladed calcite and a second silicic event where quartz replaced calcite and barite and became pervasive throughout the core. Otahal (2006) noted that chlorite occurred throughout the P3-1 core and was the most common hydrothermal clay mineral, which is consistent with our findings. The identifications noted by Otahal (2006) are shown as circles at specific depths in Fig. 8.

We identified kaolinite at only five locations within the core, at 691 ft and 812–881 ft. These occurrences of kaolinite fill gaps between minor kaolinite identified by Otahal (2006) using XRD. There are several locations where kaolinite was identified by Otahal (2006) and not in the ASD spectral survey. This is likely due to the presence of the mineral at either a very small scale, too small to be identified within our 10 mm spot size, or at a very small abundance, less than 5% of the field of view.

We identified opal at 653 and 819 ft depths, which is relatively consistent with Otahal's (2006) findings that opal was common in the P10-1 core but rare in the P3-1 core. The presence of opal at the top half of the P3-1 core could mean that temperatures were lower at shallower depths during the silicic alteration that precipitated quartz. The opal spectra near 819 ft depth had shallower 2.2 μm features than the opal at 653 ft depth, more indicative of a hydrated quartz. Otahal (2006) postulates that the P10-1 area never reached the higher temperatures of the P3-1 core during past hydrothermal events due to the abundance of opal in the P10-1 core. In hindsight

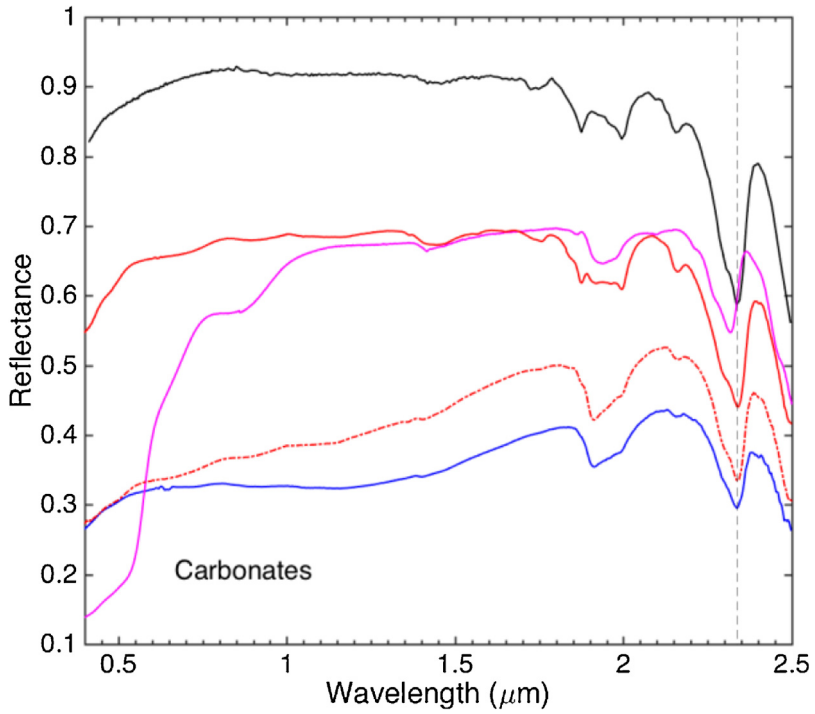

Fig. 7. Typical carbonate spectra from DB2 (blue) and HSB2 (red) cores with calcite (black) from the USGS library (Clark et al., 2007) and a dolomite (magenta) from the ASTER library (Baldridge et al., 2009).

this core was not ideal for studying alteration patterns because the both the lithology and hydrothermal alteration were essentially homogenous throughout the length of the core.

4.2. Blue Mountain (Deep Blue No. 2)

Six alteration minerals were identified from spectra collected from the Deep Blue 2 core, kaolinite, chlorite, muscovite, montmorillonite, prehnite, and calcite (Fig. 9). Kaolinite was confined to the top section of the surveyed core, at 675 ft and 1010–1141 ft depth. The geologic log by Fairbank Engineering (2004) noted kaolinite within felsic dikes at 1022–1147 ft depth, which fits well with the kaolinite we identified. Some muscovite and montmorillonite occur within the kaolinite region, which suggests argillic alteration within the felsic dikes. This is consistent with Fairbank Engineering's report that states that most of the felsic dikes are strongly argillically altered and mineralized (2004). These dikes are possibly related to local gold mineralization around hot springs that existed a minimum of 3.9 Ma (Garside et al., 1993; Fairbank Engineering, 2004).

Muscovite is observed at many deeper locations, though generally not within the diabase dikes. Fairbank Engineering (2004) acknowledges that argillic alteration looks similar to the original clay in the argillite and sandstone. Chlorite was present throughout the length of the core in every rock type, including both felsic and diabase dikes.

Prehnite was identified at one location within the core at 3236 ft depth within diabase dikes. Calcite was identified predominantly within the diabase, and montmorillonite was also present. These minerals, with chlorite, indicate propylitic alteration of the diabase dikes. Fairbank Engineering (2004) specifically noted propylitic alteration at 2485–2576 and 2689–2961 ft depths, so our interpretations expand this region of propylitic alteration a bit deeper to include the majority of the diabase unit.

We identified opal or hydrated quartz at numerous locations within the top half of the surveyed core, as shown in Figs. 1 and 9. Opal was found within argillite and sandstone. Fairbank Engineering (2004) note that silicification is the most common type of alteration, albeit difficult to distinguish from silica in the argillite and sandstone.

Consistent with the findings of Fairbank Engineering (2004) we observed argillic alteration associated with the felsic dikes near the top of the surveyed core and propylitic alteration associated with the diabase dikes in the bottom half of the surveyed core (Fig. 9). These observations suggest that hydrothermal fluids have moved along the dikes.

4.3. Akutan (HSB2)

Minerals identified using spectra collected from the HSB2 core include kaolinite, chlorite, muscovite, montmorillonite, calcite, prehnite, epidote, and zeolites (Fig. 10). Kaolinite was only identified at one location within the core, at ~60 ft depth. Muscovite was identified only at ~258 and 573 ft depths. These findings suggest argillic alteration at localized regions in the core.

Chlorite, montmorillonite, calcite, and zeolites were found throughout the core in all rock types (andesite, basalt, lithic basalt, and tuff). Prehnite and epidote were also common, though less so than other minerals. The shallowest occurrence of epidote was at ~207 ft, which is similar to the shallowest occurrence noted by Stelling and Kent (2011) at ~237 ft. The presence of chlorite, calcite, zeolites, prehnite, and epidote suggest widespread propylitic alteration; our results fill the gaps between XRD and thin section data from Stelling and Kent (2011). There is no discernible pattern to the distribution of propylitic alteration minerals, which suggests the entire depth of the well has seen hydrothermal fluid flooding. Stelling and Kent (2011) were able to identify some additional minerals that gave them insight into hotter sections of the well, including quartz, adularia, and specific zeolite species (mordenite, analcime, heulandite, chabazite, laumontite, yugawaralite, and wairakite). As discussed in Section 3.3.3, many zeolites have similar spectral shapes, making it difficult to uniquely identify them.

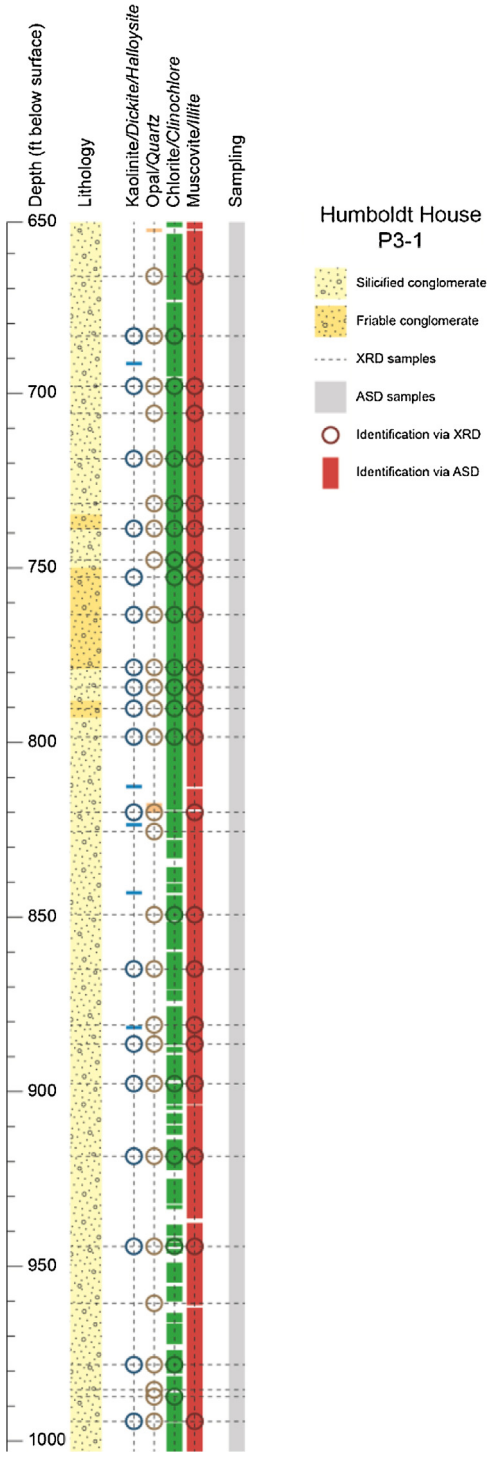

Fig. 8. P3-1 core log showing lithology and results from whole rock XRD analysis by Otahal (2006) compared with hydrothermal mineral identifications made using spectral data. Results from the spectral analysis are shown in boxes and results from Otahal (2006) are shown in circles. Italicized minerals were identified by XRD only. ASD sampling was essentially continuous, as shown by the grey box, whereas XRD sampling was sporadic, as shown by the dashed horizontal lines. Otahal (2006) identified other minor minerals in addition to the ones shown here, but these are not plotted as they are less relevant to this study.

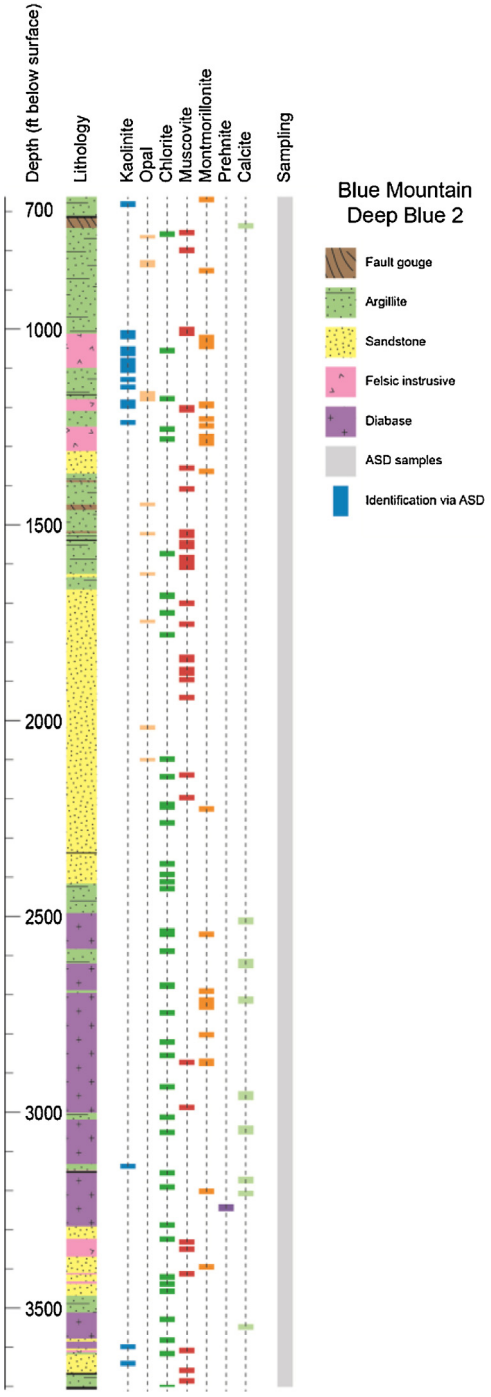

Fig. 9. Deep Blue 2 core log showing lithology logged by Fairbank Engineering (2004) compared with hydrothermal mineral identifications made using spectral data. Results from the spectral analysis are shown in boxes. ASD sampling was essentially continuous, as shown by the grey box.

5. Discussion

5.1. Pilot studies

5.1.1. Methodology and data processing

Initial data collection used an external light source and standard 8-degree field of view objective. This measurement method often creates interference "ringing" in the measured spectra, as evidenced in several of the DB2 spectra, and clearly noted in Fig. 6. Later acquisitions used the contact probe which provides a smaller field of view and more user control on the location of the spectrum collection. The contact probe works well on the outer surface or split faces of core, effectively eliminating stray light. In our studies of drill chips, we have measured samples glued on a board, in typical plastic chip trays, or on a glass sample plate (either clear or painted flat black). The glue caused significant interference with interpreting mineral spectral features (Kratt et al., 2004). Often, the

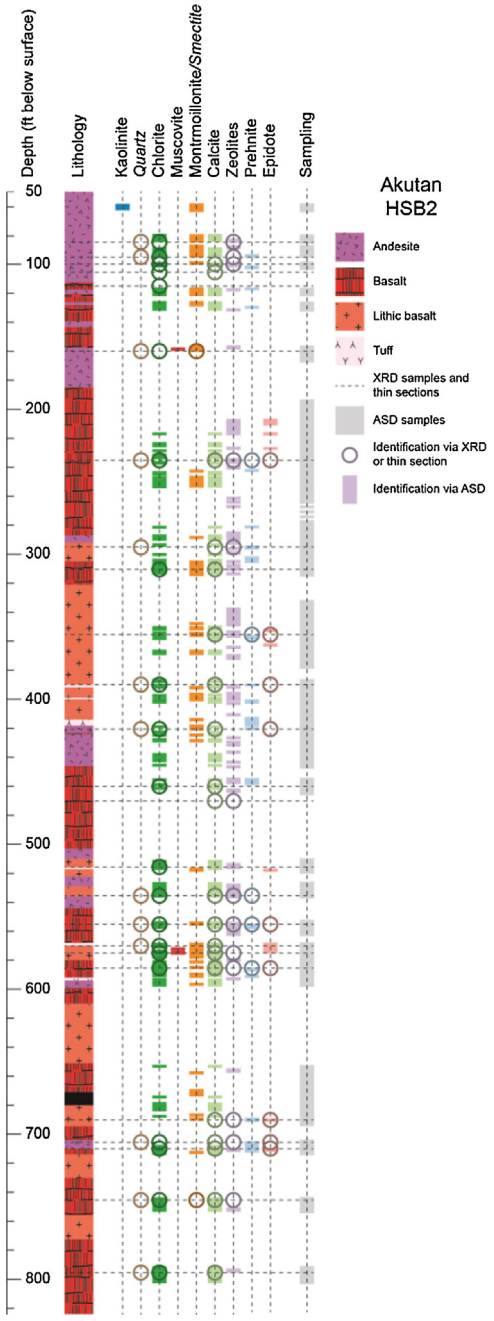

Fig. 10. HSB2 core log showing lithology and results from Stelling and Kent (2011) compared with hydrothermal mineral identifications made using spectral data. Stelling and Kent (2011) used XRD and petrographic thin sections to identify mineralogy. Results from the spectral analysis are shown in boxes and results from Stelling and Kent (2011) are shown in circles. Italicized minerals were identified by Stelling and Kent (2011) only. ASD sampling was more continuous, as shown by the grey box, than sampling for XRD and petrographic analysis, as shown by the dashed horizontal lines. Stelling and Kent (2011) identified other minerals in addition to the ones shown here and were able to differentiate between zeolite species.

contact probe does not fit into the standard chip tray section so light reflected from the surrounding tray may contribute the absorption features of the tray to the measured spectrum. We find the least interference when measuring chips by using the contact probe and having the chips on a flat sample plate, ~1 mm depth to eliminate contributions from the plate itself.

Several automated mineral identification software packages are commercially available and can provide an initial assessment of alteration mineralogy. For geothermal core we have found it useful to have a trained spectroscopist vet the data and create the final mineral map with depth.

5.1.2. Mineral identification results

We were able to identify a variety of hydrothermal alteration minerals using spectral data collected from the three cores described above: P3-1 (Humboldt House), DB2 (Blue Mountain), and HSB2 (Akutan). Alteration minerals identified included kaolinite, opal, chlorite, muscovite, illite, montmorillonite, prehnite, epidote, calcite, and zeolites. At the spatial scales used, minerals typically occur in combinations, exhibiting diagnostic features of alteration assemblages, and occasionally relatively pure mineral features. Aluminum phyllosilicates are readily identified, though the 2.2 μm kaolinite doublet is often diffuse, or expressed as an asymmetric envelope rather than a full double absorption feature. Propylitic alteration assemblages including muscovite, illite, chlorite, clinochlore, and epidote were identified with common spectral features in both the DB2 and P3-1 surveys. Mixtures of these minerals can account for a diagnostic triplet at 2.20 2.25 and 2.35 μm, though relative strength of these features varies, depending on the local concentration of minerals in the field of view. The shape of the 1.9 μm feature is diagnostic, being more boxy in chlorite and clinochlore dominated mixtures and more triangular in illite/muscovite mixtures and the addition of some smectite (montmorillonite) is also indicated with this shape. Opal and hydrated quartz veins are also apparent, and distinguished by shape and symmetry of the 1.4 and 1.9 μm water absorptions, while opal has an additional diagnostic feature at 2.2 μm. These are separable from zeolites based on the width and asymmetry of major features. Many zeolite species are not separable using infrared spectroscopy alone, so if temperature of formation of zeolites is important to understanding the geothermal field, a rapid spectral survey can be followed by more in depth analysis using higher resolution techniques. Calcite was identified in both DB2 and HSB2.

5.1.3. Comparison with traditional methods

A field portable spectroradiometer can provide rapid analysis of major core alteration minerals in near-continuous depth coverage. All of our surveys were conducted in a few days time, with preliminary assessment of primary phases occurring within approximately one week. If conducted in conjunction with geologic logging, the spectra can point to sections of the core that should be examined in more detail to understand the thermal evolution of the geothermal reservoir. In the two surveys where previous detailed petrographic and XRD work had been conducted there is very good agreement between the two techniques. We identified pervasive chlorite in P3-1, observed as the dominant alteration mineral in thin sections from that well. We identified chlorites, calcite, zeolites and prehnite at the same locations as thin section and XRD analysis in the Akutan core. Expanding on previous work, the technique provided near continuous assessment of dominant alteration minerals, filling gaps in coverage provided by a limited number of petrographic analyses. These surveys were also able to distinguish differences in phyllosilicate mineralogy simply identified as “argillic alteration” in visual inspection of the DB2 core. Common alteration assemblages (argillic, phyllic, propylitic) are readily identified and associated with fluid conduits or establishing pervasive fluid interaction throughout the core. Limitations to the technique are that some minerals of interest are not spectrally active in the VNIR/SWIR and that minor constituents may not be apparent. Augmenting a spectral survey with thin section and SEM techniques can identify very small scale or less abundant minerals. The scale of measurement is inferred to be the cause of minerals that were identified using petrographic techniques, but were not seen in our spectral surveys.

5.2. Future trends

CSIRO of Australia developed the HyLogger instrumentation to automatically scan drill core and chips (CSIRO, 2012). Similar automated instruments are operated by commercial companies including CoreScan, TerraCore/ALS Minerals, or offered as systems, e.g., Gilden Photonics (sisuRock) (the use of trade names is for descriptive purposes only and does not constitute an endorsement on the part of the authors). These automated technologies differ from our manual collection techniques but the spectral data obtained by both methods are similar. Commercial systems vary in how they image, the spatial scale of the spectral data, and the processing techniques for mineral identification. The advantage of these systems is rapid scanning of many kilometers of core at spatial scales less than 1 mm. This significantly improves the ability to map mineral associations and identify pure minerals in the assemblages that are viewed as mixtures with our field instrument and contact probe. These systems deliver true alteration logs that can be integrated with other geophysical wire-line log information such as gamma ray, seismic velocities, resistivity, and magnetic susceptibility and built into 3D geologic models using software packages such as Petrel, Leapfrog, or EarthVision. Systems are also planned that provide spectral information at longer infrared wavelengths where all rock-forming silicates (feldspars, mafic minerals) have diagnostic features.

Planned future work in our group will be to do systematic studies comparing bulk core spectra obtained at spatial scales described here with new laboratory systems that couple petrographic microscopes with the ability to collect spectral data at spatial scales of tens of micrometers. We plan to obtain multiple types of measurements, thin section and SEM data on the same samples in order to better understand the controls on which minerals dominate the bulk analysis described here.

6. Conclusions

We have demonstrated that systematic surveys using field instruments can rapidly identify the dominant alteration mineralogy in geothermal drill core. Preliminary studies helped establish reliable methods for obtaining quality data via a contact probe. A wide range of alteration minerals have been identified and mapped, with good correlation to more detailed, but spatially sparse analyses using traditional petrographic techniques. Unique spectral shapes characterize the mineral mixtures that are observed at the 10 mm spatial scale, and these shapes are common across the three sites we surveyed. Future exploration should consider this type of survey to maximize downhole information and provide quick assessment of sections of the core where more detailed study would be desirable.

Acknowledgements

We would like to thank Kim Niggemann, Gina Temple, and Pete Stelling for access to the core material in these pilot studies. Chris Kratt, Amie Lamb, Tyler Kent, and Brittany Larabee assisted with the data collection, box lugging, and heavy lifting. Nominal support for travel and some data analyses provided by DOE awards: FG36-02ID14311 and 10EE0003997 to the Great Basin Center for Geothermal Energy. Thoughtful comments from an anonymous reviewer helped to clarify the exposition.

References

Baldridge, A.M., Hook, S.J., Grove, C.I., Rivera, G., 2009. The ASTER spectral library version 2.0. Remote Sens. Environ. 113, 711–715, http://dx.doi.org/10.1016/j.rse.2008.11.007.

Bishop, J.L., Lane, M.D., Dyar, M.D., Brown, A.J., 2008. Reflectance and emission spectroscopy study of four groups of phyllosilicates: smectites, kaolinite-serpentines, chlorites and micas. Clay Miner. 43, 35–54, http://dx.doi.org/10.1180/claymin.2008.043.1.03.

Bishop, J.L., Gates, W.P., Makarewicz, H.D., McKeown, N.K., Hiroi, T., 2011. Reflectance spectroscopy of beidellites and their importance for Mars. Clays Clay Miner. 59 (4), 378–399, http://dx.doi.org/10.1346/ccmn.2011.0590403.

Browne, P.R.L., 1978. Hydrothermal alteration in active geothermal fields. Annu. Rev. Earth Planet. Sci. 6, 229–250.

Calvin, W.M., King, T.V.V., 1997. Spectral characteristics of iron-bearing phyllosilicates: Comparison to Orgueil (CI1), Murchison and Murray (CM2). Meteorit. Planet. Sci. 32, 693–701, http://dx.doi.org/10.1111/j. 1945-5100.1997.tb01554.x.

Calvin, W.M., Littlefield, E.F., Kratt, C., 2015. Remote sensing of geothermal-related minerals for resource exploration in Nevada. Geothermics 53, 517–526, http://dx.doi.org/10.1016/j.geothermics.2014.09.002.

Calvin, W., Lamb, A., Kratt, C., 2010. Rapid characterization of drill core and cutting mineralogy using infrared spectroscopy. Geotherm. Res. Counc. Trans. 34, 761–764.

Calvin, W.M., Solum, J.G., 2005. Drill hole logging with infrared spectroscopy. Geotherm. Res. Counc. Trans. 29, 565–568.

Clark, R.N., Swayze, G.A., Wise, R., Livo, E., Hoefen, T., Kokaly, R., Sutley, S.J., 2007. USGS Digital Spectral Library Splib06a, Digital Data Series 231. U.S. Geological Survey, Denver, CO http://speclab.cr.usgs.gov/spectral.lib06/ds231/index.html.

Clark, R.N., King, T.V.V., Klejwa, M., Swayze, G.A., 1990. High spectral resolution reflectance spectroscopy of minerals. J. Geophys. Res. 95, 12653–12680.

CSIRO, 2012. HyLogging™ systems. Retrieved from http://www.csiro.au/Organisation-Structure/Flagships/Minerals-Down-Under-Flagship/Exploration/hylogging-systems.aspx.

Ehlmann, B.L., Mustard, J.F., Clark, R.N., Swayze, G.A., Murchie, S.L., 2011. Evidence for low-grade metamorphism, hydrothermal alteration, and diagenesis on Mars from phyllosilicate mineral assemblages. Clays Clay Miner. 59, 359–377, http://dx.doi.org/10.1346/ccmn.2011.0590402.

Ellis, R., 2011. A restated conceptual model for the Humboldt House-Rye Patch geothermal resource area, Pershing County, Nevada. Geotherm. Res. Counc. Trans. 35, 769–776.

Fairbank Engineering Ltd, 2004. Deep Blue No. 2 Geothermal Test Well GRED II Phase II—Drilling Report. Technical Report, 10.2172/887002.

Fournier, R.O., 1985. Carbonate transport and deposition in the epithermal environment, chapter 4. In: Berger, B.R., Bethke, P.M. (Eds.), Geology and Geochemistry of Epithermal Systems, Reviews in Economic Geology, vol. 2. Society of Economic Geologists, pp. 63–72.

Gaffey, S.J., 1986. Spectral reflectance of carbonate minerals in the visible and near-infrared (0.35–2.55 microns)—calcite, aragonite, and dolomite. Am. Mineral. 71, 151–162.

Gaffey, S.J., 1987. Spectral reflectance of carbonate minerals in the visible and near-infrared (0.35–2.55 μm)—anhydrous carbonate minerals. J. Geophys. Res. Solid Earth Planets 92, 1429–1440, http://dx.doi.org/10.1029/JB092iB02p01429.

Garside, L.J., Bonham Jr., H.F., Tingley, J.V., McKee, E.H., 1993. Potassium–argon ages of igneous rocks and alteration minerals associated with mineral deposits, western and southern Nevada and eastern California. Isochron West J. 59, 17–23.

Gates, W.P., 2005. Infrared spectroscopy and the chemistry of dioctahedral smectites. In: Kloprogge, J.T. (Ed.), The Application of Vibrational Spectroscopy to Clay Minerals and Layered Double Hydroxides, Clay Minerals Society Workshop Lecture Series, vol. 13. The Clay Minerals Society.

Goryniuk, M.C., Rivard, B.A., Jones, B., 2004. The reflectance spectra of opal-A (0.5–25 (m) from the Taupo Volcanic Zone: spectra that may identify hydrothermal systems on planetary surfaces. Geophys. Res. Lett. 31, L24701, http://dx.doi.org/10.1029/2004GL021481.

Guisseau, D., Mas, P.P., Beaufort, D., Girard, J.P., Inoue, A., Sanjuan, B., Petit, S., Lens, A., Genter, A., 2007. Significance of the depth-related transition montmorillonite-beidellite in the Bouillante geothermal field (Guadeloupe, Lesser Antilles). Am. Mineral. 92, 1800–1813, http://dx.doi.org/10.2138/am.2007.2398.

Gunderson, R., Cumming, W., Astra, D., Harvey, C., 2000. Analysis of smectite clays in geothermal drill cuttings by the methylene blue method: for well site geothermometry and resistivity sounding correlation. Proceedings World Geothermal Congress, 1175–1181.

Harraden, C.L., McNulty, B.A., Gregory, M.J., Lang, J.R., 2013. Shortwave infrared spectral analysis of hydrothermal alteration associated with the Pebble porphyry copper-gold-molybdenum deposit, Iliamna, Alaska. Econ. Geol. 108, 483–494, http://dx.doi.org/10.2113/econgeo.108.3.483.

Henley, R.W., Ellis, A.J., 1983. Geothermal systems ancient and modern: a geochemical review. Earth Sci. Rev. 19, 1–50, http://dx.doi.org/10.1016/0012-8252(83)90075-2.

Inoue, A., Meunier, A., Beaufort, D., 2004. Illite-smectite mixed-layer minerals in felsic volcaniclastic rocks from drill cores, Kakkonda, Japan. Clays Clay Miner. 52, 66–84, http://dx.doi.org/10.1346/CCMN. 2004.0520108.

Johnson, J.L., 2005. Characterization of Past Hydrothermal Fluids in the Humboldt House Geothermal Area, Pershing County, NV: Geochemical and Paragenetic Studies of Core Samples. (MS Thesis). University of Nevada, Reno, NV.

King, T.V.V., Clark, R.N., 1989. Spectral characteristics of chlorites and Mg-serpentines using high-resolution reflectance spectroscopy. J. Geophys. Res. 94, 13997–14008, http://dx.doi.org/10.1029/JB094iB10p13997.

Kolker, A., Stelling, P., Cumming, W., Rohrs, D., 2012. Exploration of the Akutan geothermal resource area. Stanford University Thirty-Seventh Workshop on Geothermal Reservoir Engineering Proceedings, SGP-TR-194, 10.

Kralj, P., Rychagov, S., 2010. Zeolites in volcanic-igneous hydrothermal systems: a case study of Pauzhetka geothermal field (Kamchatka) and Oligocene Smrekovec volcanic complex (Slovenia). Environ. Earth Sci. 59, 951–956, http://dx.doi.org/10.1007/s12665-009-0249-4.

Kratt, C., Calvin, W., Coolbaugh, M., 2006. Geothermal exploration with Hymap hyperspectral data at Brady–Desert Peak, Nevada. Remote Sens. Environ. 104, 313–324.

Kratt, C., Calvin, W., Lutz, S.J., 2004. Spectal analysis of well cuttings from Drillhole DP 23-1, Desert Peak EGS area, Nevada—preliminary study of minerals and lithologies by infrared spectrometry. Geotherm. Res. Counc. Trans. 28, 473–476.

Kruse, F.A., 1996. Identification and mapping of minerals in drill core using hyperspectral image analysis of infrared reflectance spectra. Int. J. Remote Sens. 17, 1623–1632.

Ledésert, B., Hébert, R.L., Grall, C., Genter, A., Dezayes, C., Bartier, D., Gérard, A., 2009. Calcimetry as a useful tool for a better knowledge of flow pathways in the Soultz-sous-Forêts Enhanced Geothermal System. J. Volcanol. Geotherm. Res. 181, 106–114, http://dx.doi.org/10.1016/j.jvolgeores.2009.01.001.

Littlefield, E., Calvin, W., Stelling, P., Kent, T., 2012. Reflectance spectroscopy as a drill core logging technique: an example using core from the Akutan geothermal exploration project. Geotherm. Res. Counc. Trans. 36, 1283–1291.

Marks, N., Schiffman, P., Zierenberg, R.A., Frannon, H., Fridleifsson, G.O., 2010. Hydrothermal alteration in the Reykjanes geothermal system: insights from Iceland deep drilling program well RN-17. J. Volcanol. Geotherm. Res. 189, 172–190, http://dx.doi.org/10.1016/j.jvolgeores.2009.10.018.

Mas, A., Patrier, P., Beaufort, D., Genter, A., 2003. Clay-mineral signatures of fossil and active hydrothermal circulations in the geothermal system of the Lamentin Plain, Martinique. J. Volcanol. Geotherm. Res. 124, 195–218, http://dx.doi.org/10.1016/S0377-0273(03)00044-1.

Mas, A., Guisseau, D., Mas, P.P., Beaufort, D., Genter, A., Sanjuan, B., Girard, J.P., 2006. Clay minerals related to the hydrothermal activity of the Bouillante geothermal field (Guadeloupe). J. Volcanol. Geotherm. Res. 158, 380–400, http://dx.doi.org/10.1016/j.jvolgeores.2006.07.010.

Newman, G.A., Gasperikova, E., Hoversten, G.M., Wannamaker, P.E., 2008. Three-dimensional magnetotelluric characterization of the Coso geothermal field. Geothermics 37, 369–399, http://dx.doi.org/10.1016/j.geothermics.2008.02.006.

Otahal, J.M., 2006. Hydrothermal Alteration of Basin Sediments and the Chemical Evolution of an Extensional Geothermal System, Humboldt House Geothermal Area, Pershing County, Nevada. (MS Thesis). University of Nevada, Reno, NV.

Ponce, D.A., Watt, J.T., Casteel, J., Logsdon, G., 2009. Physical-property measurements on core samples from drill-holes DB-1 and DB-2, Blue Mountain geothermal prospect, north-central Nevada,USGS Open file report OF 2009-1022.

Reyes, A.G., 1990. Petrology of Philippine geothermal systems and the application of alteration mineralogy to their assessment. J. Volcanol. Geotherm. Res. 43, 279–309, http://dx.doi.org/10.1016/0377-0273(90)90057-M.

Ross, P.S., Bourke, A., Fresia, B., 2013. A multi-sensor logger for rock cores: methodology and preliminary results from the Matagami mining camp, Canada. Ore Geol. Rev. 53, 93–111, http://dx.doi.org/10.1016/j.oregeorev.2013.01.002.

Silberman, M.L., Berger, B.R., 1985. Relationship of trace-element patterns to alteration and morphology in epithermal precious-metal deposits, chapter 9. Geology and Geochemistry of Epithermal Systems, Reviews in Economic Geology, vol. 2. Society of Economic Geologists, pp. 203–232.

Stelling, P., Kent, T., 2011. Akutan Geothermal Exploration Project: Geological Analysis of Drill Core Form Geothermal Gradient Wells HSB2 and HSB4. Stelco Magma Consulting Report16.

Sun, Y.Y., Seccombe, P.K., Yang, K., 2001. Application of short-wave infrared spectroscopy to define alteration zones associated with the Elura zinc-lead-silver deposit, NSW, Australia. J. Geochem. Explor. 73, 11–26, http://dx.doi.org/10.1016/s0375-6742(01)00167-4.

Tappert, M., Rivard, B., Giles, D., Tappert, R., Mauger, A., 2011. Automated drill core logging using visible and near-infrared reflectance spectroscopy: a case study from the Olympic Dam IOCG deposit, South Australia. Econ. Geol. 106, 289–296, http://dx.doi.org/10.2113/econgeo.106.2.289.

Tappert, M.C., Rivard, B., Giles, D., Tappert, R., Mauger, A., 2013. The mineral chemistry, near-infrared, and mid-infrared reflectance spectroscopy of phengite from the Olympic Dam IOCG deposit, South Australia. Ore Geol. Rev. 53, 26–38, http://dx.doi.org/10.1016/j.oregeorev.2012.12.006.

Taylor, G.R., 2000. Mineral and lithology mapping of drill core pulps using visible and infrared spectrometry. Nat. Resour. Res. 9, 257–268, http://dx.doi.org/10.1023/A: 1011501125239.

Thompson, A.J.B., Hauff, P.L., Robitaille, A.J., 1999. Alteration mapping in exploration: application of shortwave infrared (SWIR) spectroscopy. Soc. Econ. Geol. Newslett. 39, 16–27.

Yang, K., Huntington, J.F., Browne, P.R.L., Ma, C., 2000. An infrared spectral reflectance study of hydrothermal alteration minerals from the Te Mihi sector of the Wairakei geothermal system, New Zealand. Geothermics 29 (3), 377–392, http://dx.doi.org/10.1016/s0375-6505(00)00004-3.

Yang, K., Browne, P.R.L., Huntington, J.F., Walshe, J.L., 2001. Characterising the hydrothermal alteration of the Broadlands–Ohaaki geothermal system, New Zealand, using short-wave infrared spectroscopy. J. Volcanol. Geotherm. Res. 106, 53–65, http://dx.doi.org/10.1016/s0377-0273(00)00264-x.

Yang, K., Huntington, J.F., Gemmell, J.B., Scott, K.M., 2011. Variations in composition and abundance of white mica in the hydrothermal alteration system at Hellyer, Tasmania, as revealed by infrared reflectance spectroscopy. J. Geochem. Explor. 108 (2), 143–156, http://dx.doi.org/10.1016/j.gexplo.2011.01.001.